

SIMULATION OF A SOLIDS FREE DRILL-IN FLUID INVASION THROUGH OIL RESERVOIR ROCKS

André Leibsohn Martins

PETROBRAS- Cidade Universitária, Q7 – Ilha do Fundão – Prédio 20 – Sala 1017 – Rio de Janeiro-RJ

CEP: 21941-598

aleibsohn@petrobras.com.br

Alex Tadeu de Almeida Waldmann

PETROBRAS- Cidade Universitária, Q7 – Ilha do Fundão – Prédio 20 – Sala 1017 – Rio de Janeiro-RJ

CEP: 21941-598

waldmann.puc@petrobras.com.br

Daniel da Cunha Ribeiro

Rodovia SC 401, km 001 – Saco Grande – Florianópolis-SC

CEP: 88030-000

daniel@esss.com.br

Giulio Massarani (*in memoriam*)

Abstract. *Designing drill in fluids which can guarantee minimum invasion into the reservoir rock is a must for open hole completion wells. The industry has proposed several ideas to deal with the problem, most of them based on adding bridging agents to the fluid formulation. Such agents would block pores near the well bore and, consequently, prevent additional fluid to invade the rock, but often require acid treatment for their removal.*

A different concept is proposed for controlling invasion in this article: designing a polymer based fluid which would generate extremely high friction losses when flowing through a porous media without generating extra losses while flowing in the well. In this case the fluid would present proper flow and solids transport properties in the well and would not invade the rock formation.

Based on a viscoelastic resistive force proposition for the porous media, flow characterization maps defining viscous flow, elastic flow and viscoelastic flow regions are obtained. The invasion analysis is based on a 2 phase (viscoelastic fluid + Newtonian oil) radial flow through porous media and supported by a commercial CFD package.

Keywords: *Two phase flow, CFD, simulation, fluid, drilling*

1. Introduction

In petroleum engineering, well drilling is an area of continuous development in order to improve the current technologies and look for new ones which can be applied to the adverse conditions faced nowadays and enable operations that were only conceptual some decades ago.

Oilwell drilling involves costly operations where avoiding reservoir damage and minimizing operational time are very important issues. The drilling operation generally occurs through weight and rotation of a string which extremity is connected to a bit. Simultaneously, a drilling fluid is circulated through the well according to the following path: the fluid is injected into the column, passes through the bit nozzles and returns through the annular space formed by the wellbore and drilling column. Figure 1 highlights the fluid circulation scheme.

Different types of fluid are used in the several the drilling phases of an offshore well. In its initial phases, the well is drilled without fluid return, with sea water or water with clay when higher densities are required. Extended and high angle sections are normally drilled with fluids based on synthetic oils with good lubricity and low reactivity with shales. Reservoir rocks are drilled with a fluid family known as drill-in, composed by saline polymeric solutions with bridging agents.

One of the drilling fluid basic functions is to exert hydrostatic pressure over the permeable formations to avoid the formation fluid invasion to the well while the drilling operation takes place. The fluid pressure is normally kept above the formation pore pressure to prevent from kick events (formation fluid invasion to the well), that, in some cases, can lead to an uncontrolled influx (blowout). This concept, called overbalanced drilling, is traditionally employed in most of the drilling operations worldwide and in Brazil.

As the bit penetrates the reservoir rock, the drilling fluid invades the formation due to the positive pressure differential between the well and the reservoir rock. Portions of the liquid phase of the drilling fluid are lost to the adjacent formation while part of the solids presented in drilling fluid, constituted by particles smaller than the formation pore size, penetrate the rock during the fluid loss period, rapidly plugging the region around the well (Fig 2). Larger particles accumulate on the wellbore walls, initiating an external cake formation. The invasion of fluid and solid particles during this process cause damage to formation around the well.

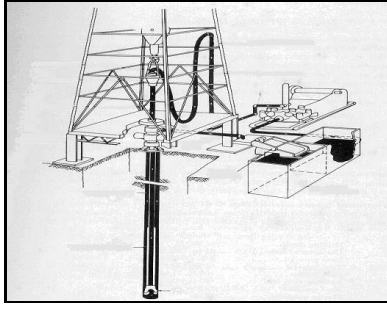


Figure 1. Fluid circulation system

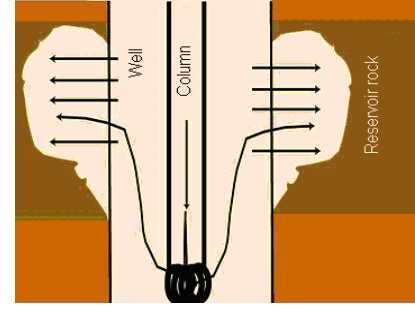


Figure 2. Drilling fluid invasion in reservoir rock

Two invasion mechanisms are notable in the well. The first, called filtration, occurs when the fluid pumping is interrupted and, from that point on, filtration occurs due to the difference between the hydrostatic pressure in the well and the reservoir pressure. The filtration rates are controlled by the continuously increasing thickness of the filter cake. This mechanism is known as static filtration in Petroleum Engineering.

The other invasion mechanism, called cross filtration, occurs when the fluid is pumped through the well. In this process, the cake thickness is resultant from the dynamic equilibrium between solid particles deposition rate and the erosion rate due to the shear stresses generated by the fluid flow in the wellbore. Thus, the filtration rate to the formation tends to stabilize around a certain value while the cake thickness turns constant. This process is known as dynamic filtration in Petroleum Engineering. The invasion phenomenon approach must regard both mechanisms.

Additionally, it is relevant to note that fluid invasion implies in the displacement of the fluids saturating the reservoir rock: hydrocarbons in gas or liquid phase and water.

Two mechanisms of invasion control are identified: one through the plugging solids that promote the external and internal cake formation and other through the liquid phase resistance to the flow in porous medium. The last one is the proposed topic of this study:

Considering a constitutive equation which describes the resistive forces resultant from the flow of a Newtonian fluid through porous media, the radial two phase flow which characterizes the problem is analyzed.

2. Problem Statement

Consider a non newtonian fluid flowing through an annular space limited by the wellbore (permeable) and the drillstring (impermeable). The drillstring rotates in the hole as a result of the interaction of the fluid–structure system. As pumped, the fluid carries to the surface the solids generated by the bit. The annulus can present different inclination angles, according to the defined well path. This flow generates a pressure profile in the wellbore that will force the radial flow of fluid through the rock formation. The formation is an anisotropic porous medium saturated by a multicomponent mixture composed by liquid, gaseous hydrocarbons and water. Besides fluid composition and properties, the pressure initial distribution in the rock formation depends on the superposed stratigraphic column and on the effect of neighbor wells. Certainly, it is a complex problem which global understanding should consider simplification stages.

The representation of the phenomena that govern the solids free drilling fluid invasion into a reservoir rock will be simplified, in the present analysis, to a coupling of two distinct flows that constitute the classical problem of the cross filtration.

- The non newtonian fluid flow through a porous wall pipe;
- The radial flow of the filtrated fluid (from now on called invader fluid) from the pipe walls through the porous medium saturated by a newtonian fluid (from now on called resident fluid). The driving force for this flow is the pressure differential between internal and external surfaces of the porous wall.

The following formulation (proposed by SCHEID et al., 2000), connects pipe pressure drop with axial flow rate and invasion flow rate.

- Material balance in the pipe cross section

$$-\frac{dQ_A}{dz} = p \cdot D_i \cdot q \quad (1)$$

- Movement equation for the fluid inside the pipe

$$Q_A(z) = \frac{p}{128} \cdot \frac{D_i^4}{(m_{ef})_A} \cdot \left(-\frac{dP}{dz} \right) \quad (2)$$

where,

$$(m_{ef})_A = \frac{S(I^*)}{I^*} \quad (3)$$

Considering I^* as the characteristic shear rate inside the pipe, defined by:

$$I^* = \frac{25,6}{p} \cdot \frac{Q_A}{D_i^3} \quad (4)$$

The movement equations for fluids (invader and resident) through porous medium are:

$$- \text{grad } P_1 + \gamma_1 \cdot \mathbf{g} = \mathbf{m}_1 \quad (5)$$

$$- \text{grad } P_2 + \gamma_2 \cdot \mathbf{g} = \mathbf{m}_2 \quad (6)$$

Both former equations represent the situation where the matrix pores are filled by two immiscible fluids, as presented by MASSARANI (1997).

The resistive forces for each phase can be described, from MARTINS et al. (2004) to polymeric solutions (phase 1) and from Darcy Law to oil (phase 2)

$$m_1 = \frac{M \cdot q^n}{k_1^{\frac{n+1}{2}}} \cdot \left[1 + C_i \cdot \frac{M_i}{M} \cdot \left(\frac{q}{\sqrt{k}} \right)^{n_i - n} \right] \quad (7)$$

$$m_2 = \frac{q \cdot m}{k_2} \quad (8)$$

where k_1 and k_2 represent the relative permeability of each phase and depends on the imbibition–draining cycle of the porous matrix structure (SCHEIDEGGER, 1963). The parameters (M_1/M) and (n_1/n) are calculated based the power law coefficients for the shear and extensional material functions which the authors claim to govern the process.

The effective viscosity for both phases can be defined by:

$$(m_{ef})_{PM} = \frac{S(I^*)}{I^*} \quad (9)$$

Where the viscosity should be evaluated at the characteristic deformation rate, defined by Massarani as:

$$I^* = \frac{\|q\|}{k^{\frac{1}{2}}} \quad (10)$$

3. Filtration - Simulation

To represent this problem, the geometry shown in Figure 3 was selected:

- Wellbore diameter: 8,5 pol
- Reservoir diameter: 2 m
- Reservoir height: 1 m

Due to the tangencial geometry, it seems reasonable to define a simulation geometry with an angular section of the solid presented in Figure 3. This strategy allows to reduce the computational effort, once it reduces the number of points and transform the three-dimensional problem to one-dimensional problem. To validate this strategy, solids representing the total geometry and a 1 degree section were generated.

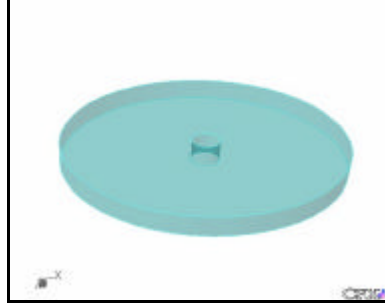


Figure 3. Geometry selected to simulate the flow in the well reservoir boundary

The simulations presented were performed from the follow base-case:

- Wellbore pressure: 560 PSI
- Reservoir pressure: zero
- Reservoir permeability: 750 mD
- Viscosity parameters:
 - $n = 0,4$
 - $M = 0,02 \text{ Pa.s}^n$
- Normal tensions parameters:
 - $n_1 = 0,9$
 - $M_1 = 0,02 \text{ Pa.s}^{n_1}$

Two forms of performing the problem are presented:

Single phase flow: in this case, the fluid inside the well invades the porous rock saturated by the same fluid. The solution of the steady state problem produces velocity fields. The propagation of the invasion front can be evaluated trough the movement of a fluid molecule or trough the movement of a tracer a long the time (Santos 1990). This strategy requires the solution of the transient problem. Once the comparisons of both results showed they were identical, the first strategy was adopted.

The boundary conditions of the problem are the pressure in the wellbore and the pressure in the reservoir. The pressure difference between the wellbore and the reservoir is the drive force of the flow.

The ratio between the real diameters of the wellbore and the reservoir is different from the simulated ratio. But the idea of the present work is to analyze the neighborhood of the well where the reservoir experiment pressures fluctuation. The initial conditions are fluid velocity in the porous medium equal to zero and pressure equal to external boundary condition.

Two phase flow: in this kind of flow, the fluid in the wellbore (invader fluid) penetrates the porous medium saturated by another fluid (resident fluid). This situation tries to approach the real case, where the drilling fluid invades the reservoir saturated by oil. This is a transient problem, once it is a fluid substitution. The propagation of the invasion front is monitored by the volumetric fraction of the invader fluid.

New initial conditions are required: in each point of the reservoir, the volumetric fraction of the invader fluid is zero and the volumetric fraction of the resident fluid is 1.

A homogeneous two phase model was used. The model considers that besides the pressure field, the velocity field is also shared.

3.1 Simulation of the single phase flow

This analysis aims to validate the methodology of the numeric solution of the radial flow. The proposal is to compare the numeric solutions with the analytic solutions presented by Martins (2004) for the Newtonian and non-newtonian fluid. The invasion ratio can be expressed as a time function as follows:

$$\Delta P = \left(\frac{R_{inv}^2 - R_i^2}{2t} \right)^n \frac{R_e^{1-n} - R_i^{1-n}}{1-n} \frac{M f^n}{k^{\frac{n+1}{2}}} + \left(\frac{R_{inv}^2 - R_i^2}{2t} \right)^{n_1} \frac{R_e^{1-n_1} - R_i^{1-n_1}}{1-n_1} \frac{C_1 M_1 f^{n_1}}{k^{\frac{n_1+1}{2}}} \quad (11)$$

Additionally, this work aims to discuss the radial profile of important variables. Table 1 shows the adequacy of the numeric solution for several invasion times.

Table 1. Adequacy of the numeric solution for several invasion times

Darcy Flow – Newtonian flow				
Result	R_{inv} (m)	Time (s)	R_{inv} (m)	Time (s)
Numeric	0,500	2800	0,900	7790
Analytic	0,506	2800	0,900	7760
Darcy Flow – Power Law flow				
Result	R_{inv} (m)	Time (s)	R_{inv} (m)	Time (s)
Numeric	0,500	1	0,900	2,7
Analytic	0,508	1	0,900	2,7
Non-darcy flow – Resistive force considering N_1				
Result	R_{inv} (m)	Tempo (s)	R_{inv} (m)	Tempo (s)
Numeric	0,500	86	0,900	241
Analytic	0,510	86	0,900	237

Once the methodology was validated, the intention is to extend the sensibility analysis to the viscoelastic flow through the numerical simulation. Table 2 highlights the velocity and viscosity profiles for different values of parameter.

Table 2. Velocity and viscosity profiles for different values of parameter

Non-darcy flow			
$(n_1 - n = 0.5)$			
	$M_1/M = 10^{-5}$	$M_1/M = 1$	$M_1/M = 10^5$
q (m/s)	1,8E-1 -1,8E+0	2,6E-3 - 2,1E-2	6,0E-9 - 7,1E-8
μ (Pa.s)	3,2E-6 - 1,3E-5	7,3E-3 - 9,2E-3	2,6E+3 -3,3E+3
Non-darcy flow			
$(M_1/M = 1)$			
	$n_1 - n = 0.5$	$n_1 - n = 1$	$n_1 - n = 1.5$
q (m/s)	2,6E-3 - 2,1E-2	7,9E-5 - 9,1E-4	1,8E-5 - 1,9E-4
μ (Pa.s)	7,3E-3 - 9,2E-3	1,2E-1 - 3,2E-1	3,0E-1 -2,5E+0

3.2 Two phase flow simulation

The methodology for the two phase flow was validated through the execution of cases where the resident and invader fluids presented the same properties and the results were compared with the identical single phase simulation results. Figure 4 highlights the invasion front evolution for the Darcy flow of a power law fluid in several times.

The invasion front, at a certain time, is indicated in the figures by the red color region end. Figure 5 highlights the analogous profiles for resistive force proposed by Equation 7. Results indicate the huge invasion control caused by the additional term.

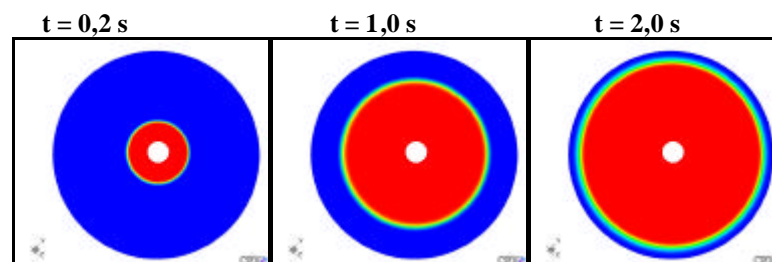


Figure 4 – Invasion front – Darcy flow (power law model fluid)

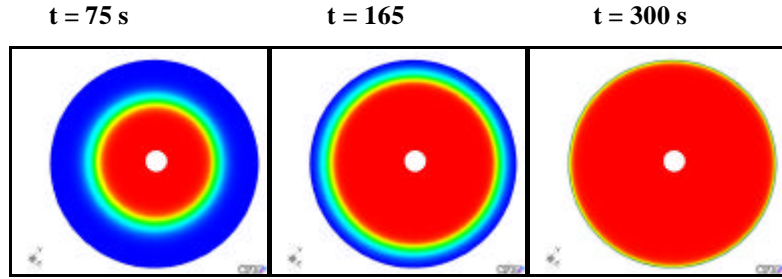


Figure 5 – Invasion front – non Darcy

The following figures aim to identify the impact of the invader and resident fluid viscosities relation in the invasion front evolution. Figures 6 and 7 highlight the results of invasion front rate for the two resistive force models in a certain time considering several viscosities for the resident fluid.

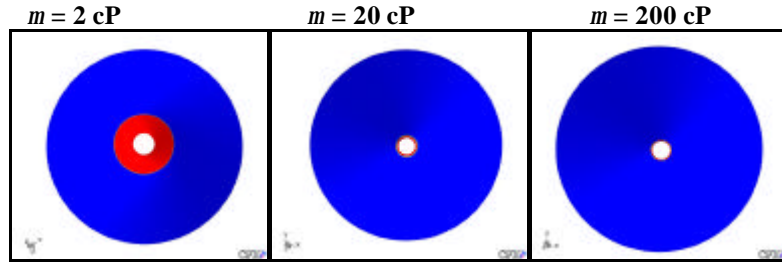


Figure 6 – Viscosity effect of the resident fluid in invasion front – Darcy Flow – time = 60 s

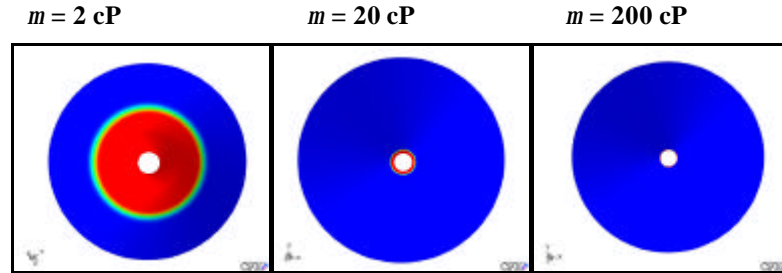


Figure 7 – Viscosity effect of the resident fluid in invasion front – Non – Darcy Flow – time = 100 s

The impact of these variations in the resident fluid properties is detailed for several polymeric invader fluids in Table 3. Again, the values highlight the potential of the additional resistive force term in the invasion control. The adoption of the homogeneous two phase modeling is limited, specially for the case where the resident fluid is more viscous than the invader one (there will be a clear tendency to fingering).

Table 3 – Viscosity effect of the resident fluid – additional resistive force model

NON DARCY FLOW (VISCOELASTIC RESISTIVE FORCE $M_1/M = 1$)			
m_{Resident}^2 (cP)	$n_1 - n = 0.5$	$n_1 - n = 1$	$n_1 - n = 1.5$
	q (m/s)	q (m/s)	q (m/s)
2	6.72E-4 - 6.73E-3	3.16E-4 - 3.19E-3	1.70E-5 - 1.87E-4
20	6.33E-5 - 6.39E-4	6.30E-5 - 6.31E-4	5.27E-5 - 5.34E-4
200	6.27E-6 - 6.34E-5	6.27E-6 - 6.34E-5	6.27E-6 - 6.34E-5
NON DARCY FLOW (VISCOELASTIC RESISTIVE FORCE $n_1 - n = 0.5$)			
m_{Resident}^2 (cP)	$M_1/M = 10^{-5}$	$M_1/M = 1$	
	q (m/s)	q (m/s)	
2	6.71E-4 - 6.94E-3	6.32E-4 - 6.73E-3	
20	6.36E-5 - 6.45E-4	6.33E-5 - 6.39E-4	
200	6.27E-6 - 6.35E-5	6.27E-6 - 6.34E-5	

3.3 Cross filtration simulation

This topic defines a domain that includes the well and the reservoir. The selected geometry for the simulations is represented in Figure 8. A 15 degree angled section was considered due to the two-dimensional nature of the problem.

The boundary conditions for the problem are the well and reservoir outlet pressures prescription. Additionally, either well inlet pressure or the flow rate is prescript associating a velocity profile related to the invader fluid rheological model (power law).

$$n(r) = \left(\frac{3n+1}{n+1} \right) \cdot \frac{Q}{A} \cdot \left(1 - \frac{r}{R_i} \right)^{\frac{n+1}{n}} \quad (12)$$

The initial conditions are the fluid velocity equal to zero in the reservoir and flow rate equal to the inlet on the well. The pressures in reservoir are initialized with the external boundary condition and in the well, with the outlet pressure.

The simulations presented as follow were performed from the same basic case used in filtration simulations. The used flows will be defined just ahead. The simulations presented in this item will be limited to the single phase case, where the resident and invader fluids have the same properties.

The following grid was considered: 123680 nodes (97x82x16), 113918 elements (1106 prisms and 112812 hexahedrons) and 22476 faces; expansion rate of 1.2 and aspect ratio of 110. The Figure 9 highlights the employed grid.

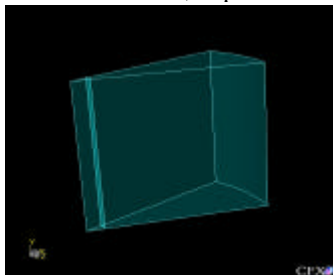


Figure 8. Schematic representation of the 15 degree angled section

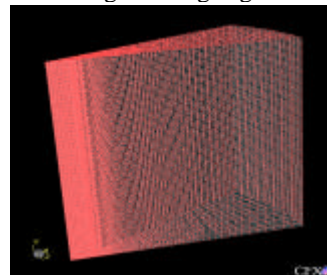


Figure 9. Employed grid for crossed filtration simulation

Initially, simulations were performed aiming the validation of the cross filtration results in relation to the ones obtained in the filtration simulations under the same conditions. In order to perform these simulations, a low fluid flow rate was used to generate a negligible axial pressure differential when compared to the radial. Thus, the filtration and the cross filtration results must be similar. Table 4 shows the comparisons in several prescript boundary conditions for a fixed case. The last line of the table represents the filtration simulation. The results indicate that the pressure drop effect in the well has a low impact in the radial invasion of the solids free fluid for the operational reality, where the radial pressure differential is of superior order of magnitude when compared to the axial).

Table 4 – Impact of the axial flow in radial invasion

Boundary conditions			Reservoir inlet velocity (x10 ⁻⁴ m/s)	Reservoir outlet velocity (x10 ⁻⁵ m/s)
Well inlet	Well outlet	Reservoir outlet		
P = 560.081psi	P = 560psi	P = 0	5.753	5.637
P = 560.0001psi	P = 560psi	P = 0	5.751	5.638
Q = 100 gpm	P = 560psi	P = 0	5.752	5.637
Q = 1gpm	P = 560psi	P = 0	5.753	5.637
NA	P = 560psi	P = 0	6.300	5.608

NA – not applicable

Simulations where the axial and radial pressure differentials are of the same order of magnitude are presented. Two simulations are illustrated: one for the Darcy flow with newtonian fluid and other for the non Darcy resistive force flow. A very high permeability was considered to illustrate the invasion (7.5E-05 m²). The considered boundary conditions were:

- Well inlet pressure: 1.0E-04 psi
- Well outlet pressure: zero
- Reservoir outlet pressure: zero

The results illustrated in Figures 10 and 11 represent the position, at different times, of a particle that invades the porous medium. In Figure 10 (newtonian fluid), the particle positions are marked from 10 to 310 s, in intervals of 100 s. In Figure 11 (polymeric fluid with $(n_1 - n) = 1.5$ and $(M_1/M) = 1$), the particle positions reflect times from 10 to 2010 s with 100 s intervals.

The results highlight the invasion axial profile in the reservoir for the situation where the axial and radial pressure differentials are of the same order of magnitude. Invasion comparisons between both fluids are not pertinent due to their distinct viscosities. These results are illustrative and confirm the hypothesis that for the solid free fluid filtration phenomenon simulation and experimentation strategy is correct due to the filtration and cross filtration results are equivalent for cases that reflect the operational reality (where the axial pressure differential is of a lower order of magnitude when compared to the radial).

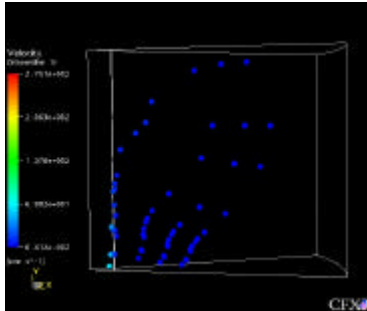


Figure 10 – Axial profile of the invasion in the reservoir – Newtonian fluid

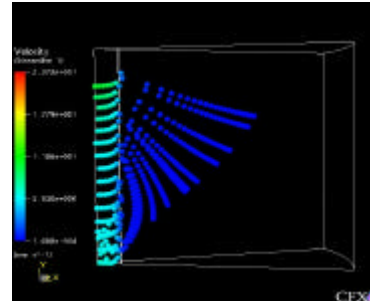


Figure 11 – Axial profile of the invasion in the reservoir – Polymeric fluid

4. Final Remarks

- The numeric methodology proposed for single phase flow simulation is adequate, once the analytical results are in accordance with the numerical solution.
- The simulations performed highlight the effectiveness of the additional resistive force on the control of reservoir invasion for representative situations of application of technology.
- This work constitutes a basic tool for the design of non-invasive fluids with no solids. It is possible to design fluids with predominance of elastic effects when flowing in porous medium. This way, the fluid would generate high friction losses without changes in its behavior in the well.
- The definition of the rheological properties to achieve this target depends on several factors, such as the well and reservoir pressures and the permeability of interest zones. Thus, the design of the non invasive fluid should be specific for each group of applications and should also consider the time the fluid and formation will be in contact.

5. References

- CHAUVETEAU, G., MOAN, M., MAGUEUR, A., “*Thickening Behaviour of Dilute Polymer Solutions in Non-Internal Elongation Flows*”, Journal of Non-Newtonian Fluid Mechanics, Vol. 16, pp. 315-327, 1984.
- CHIAPPA, L., MENELLA, A., LOCKHART, T. P., BURRAFATO, G., “*Polymer Adsorption at The Brine/Rock Interface: The Role of Electrostatic and Wettability*”, Journal of Petroleum Science and Eng., Vol. 24, pp. 113-122, 1999.
- MARTINS, A.L. (2004), Quantificação das Forças Resistivas na Escoamento de Soluções Poliméricas em Meios Porosos e seu Impacto na Engenharia de Poços de Petróleo, Dissertação de Tese de Doutorado, Universidade Federal do Rio de Janeiro, (UFRJ), COPPE/UFRJ, 192p.
- MARTINS, A. L., SILVA TELLES, A., MASSARANI, G. (2004) “Efeito de Tensões Normais no Escoamento de Fluidos Não Newtonianos em Meios Porosos”, Anais do XXXI Encontro Sobre o Escoamento em Meios Porosos, Uberlândia, MG.
- MARTINS, A.L., WALDMANN, A.T.A., ARAGÃO, A.F.L., et al., 2004, “Predicting and Monitoring Fluid Invasion in Exploratory Drilling”. In: SPE International Symposium and Exhibition on Formation Damage Control, SPE 86497, Lafayette, USA, 18-20 February.
- MASSARANI, G., SILVA TELLES, A. “*An Extended Capillary Model for Flows in Porous Media*”, Journal of Porous Media, Vol. 4, n.4, p.297-307, 2001.
- MASSARANI, G. (2002), Fluidodinâmica em Sistemas Particulados, E-Papers, Rio de Janeiro, RJ, 2ª Edição, pp.151.
- SANTOS, R.L.A. (1990), “Estudo de Injeção de Traçadores em Meios Porosos através do Método de Diferenças Finitas com Discretização Exponencial”, Dissertação de Tese de Mestrado, Unicamp, Campinas, SP, Brasil
- SCHEIDEGGER, A.E., 1963, “The Physics of Flow Through Porous Media”, University of Toronto Press, Toronto, pp. 313.

Symbols

Q_A	Flow rate (L^3/T)
Z	Position (L)
D_i	Diameter of the well (L)
μ_{ef}	Effective viscosity (M/LT)
A	Cross section area (L^2)
S	Shear stress (M/LT ²)
$\dot{\gamma}$	Shear rate (T ⁻¹)
P	Pressure (M/TL ²)
P_1	Pressure at the position 1 (M/TL ²)
P_2	Pressure at the position 2 (M/TL ²)
G	Gravity (M/T ²)
m_1	Resistive force for phase 1 (M/L ² T ²)
m_2	Resistive force for phase 2 (M/L ² T ²)
ρ_1	Phase 1 density (M/L ³)
ρ_2	Phase 2 density (M/L ³)
M	Consistence index (M.T ⁿ⁻¹ /L)
N	Behavior index (dimensionless)
K_1	Permeability of the phase 1 (L ²)
K_2	Permeability of the phase 2 (L ²)
C_i	Adjust coefficient (dimensionless)
t	Time (T)
ϕ	Porosity (dimensionless)
r	Ratio (L)
v	Velocity (L/T)